Aeromagnetic and Resistivity Surveying for Delineating Optimal Sites for Groundwater development in part of Minna, Sheet 164 SW, North-Central Nigeria

Abdullahi, D.S and Ejepu, J.S

Department of Geology, School of Physical Sciences, Federal University of Technology, Minna, Niger State, Nigeria.

*Corresponding Author: abdullahisolomondan@yahoo.com. Tel: +2348051773961

ABSTRACT

This study was conceptualised out of a need to help stem the continuous rising incidences of failed and abandoned wells in the study area. This situation is attributable to inadequate understanding of the hydrogeological and structural disposition of the area. The study area is underlain by crystalline rocks belonging to the Basement complex of Nigeria. These rocks comprise of Schist, Gneiss, Quartzite and Granite with minor occurrences of alluvial deposits. Analysis and interpretation of the Aeromagnetic data was used to map previously known and unknown fractures which are deemed to aid appreciable flow of water to drilled wells. These fractures, especially the near surface fractures were validated using interpreted VES data. The interpretation of the Vertical Electrical Sounding (VES) data was done following a calibration of various geoelectric layers from existing wells. Principal joint directions on the surface yielded primarily NE – SW trend while aeromagnetic data revealed lineaments trending principally in the ENE – WSW direction. These orientations correlate well with the general orientation of structures in the Basement Complex. VES data revealed three to four geoelectric layers comprising of the top soil at depths between 1 to 7 m and resistivity values in the range of 100Ωm to 300Ωm. This is followed by the weathered layer (for 3-layer system) or fractured layer (for 4-layer system). The last layer is the fresh basement rock of infinite resistivity. The weathered layers are generally shallow and have thicknesses in the range of 3 and 30 m while the weathered/fractured zone are the conductive layers which most likely are aquiferous. Optimal sites are delineated where the Aeromagnetic lineaments and surface structures intersect and where an appreciable thickness of the weathered layer is delineated. This study has been able to establish another zone of the aquiferous unit beyond the 200 m depth. The outcome of this research has been able to establish the need for both geological and hydrogeological investigations and the need to integrate at least two geophysical methods in groundwater exploration efforts in the Basement Complex.

Keywords: *Aeromagnetic data, Aeromagnetic Lineaments, Vertical Electrical Sounding, Fractured aquifer, groundwater exploration , Basement Complex.*

1.0 INTRODUCTION

The usual practice of groundwater exploration in Nigeria is based only on employing Vertical Electrical Sounding geophysical survey technique. Drill sites are chosen based on anomalies identified from the results of the survey often with little or no understanding of the interpretation methods, peculiarity of interpreted data, ambiguity in interpreting the results and

on the structural geology of the target area leading to high rates of unsuccessful drilling campaigns (Ejepu, 2017).

As the demand for groundwater grows, it can be expected that further development will have to consider alternative targets in such problematic and complex fractured geological environments. Hence, in order to improve the borehole success rate in these terrains and to develop groundwater resources in a sustainable manner, an integrated approach is needed. This approach must incorporate an understanding of the structural geology and its influence on the occurrence of groundwater and identification of appropriate methods and interpretative techniques so that target features can be identified in the field (Ejepu *et al.*, 2015). The aim of this research is to investigate the potential of groundwater development in the crystalline basement complex of Minna, north-central Nigeria by utilising integrated methods involving detailed geologic and structural mapping, aeromagnetic data and vertical electrical sounding techniques in order to identify geological and structural controls of groundwater in the area. Specific objectives include:

1. Analysis and interpretation of aeromagnetic anomalies for the purpose of delineating subsurface geologic structures, depth to causative bodies and their orientations.
2. Conduct Vertical Electrical Sounding in order to confirm the correctness of delineated magnetic lineaments of the area.
3. Production of a geological map on the scale of 1:25,000 with superimposed surface structural orientations on different rock units.
4. Production of groundwater potential map of the area.

2.0 Study Area

The study area is within Chanchaga, Bosso Local Government Area of Niger State, north-central Nigeria. It lies in the south-western portion of Minna Sheet 164. The study area is bounded within Latitudes 9° 32′00′′ N and 9° 34′00′′ N and Longitudes 6° 34′00′′ E and 6° 36′00′′ E. It covers a total area of about 14 km^2 (Figure 1).

The climate of the study area is that of a typical guinea savannah. There are two seasons associated with the climate; these include the rainy and dry seasons. The average total annual rainfall in this area is about 1300 mm and spreads over the months of April and October with the highest amount of rainfall being recorded between the months of August and September.

(NIMET, 2017). The area is drained mainly by River Gurara. The tributaries of the river system include rivers Gudna, Jedna, Jednadalaso, Kudan and Jatau. The drainage of the area is lithologically and structurally controlled.

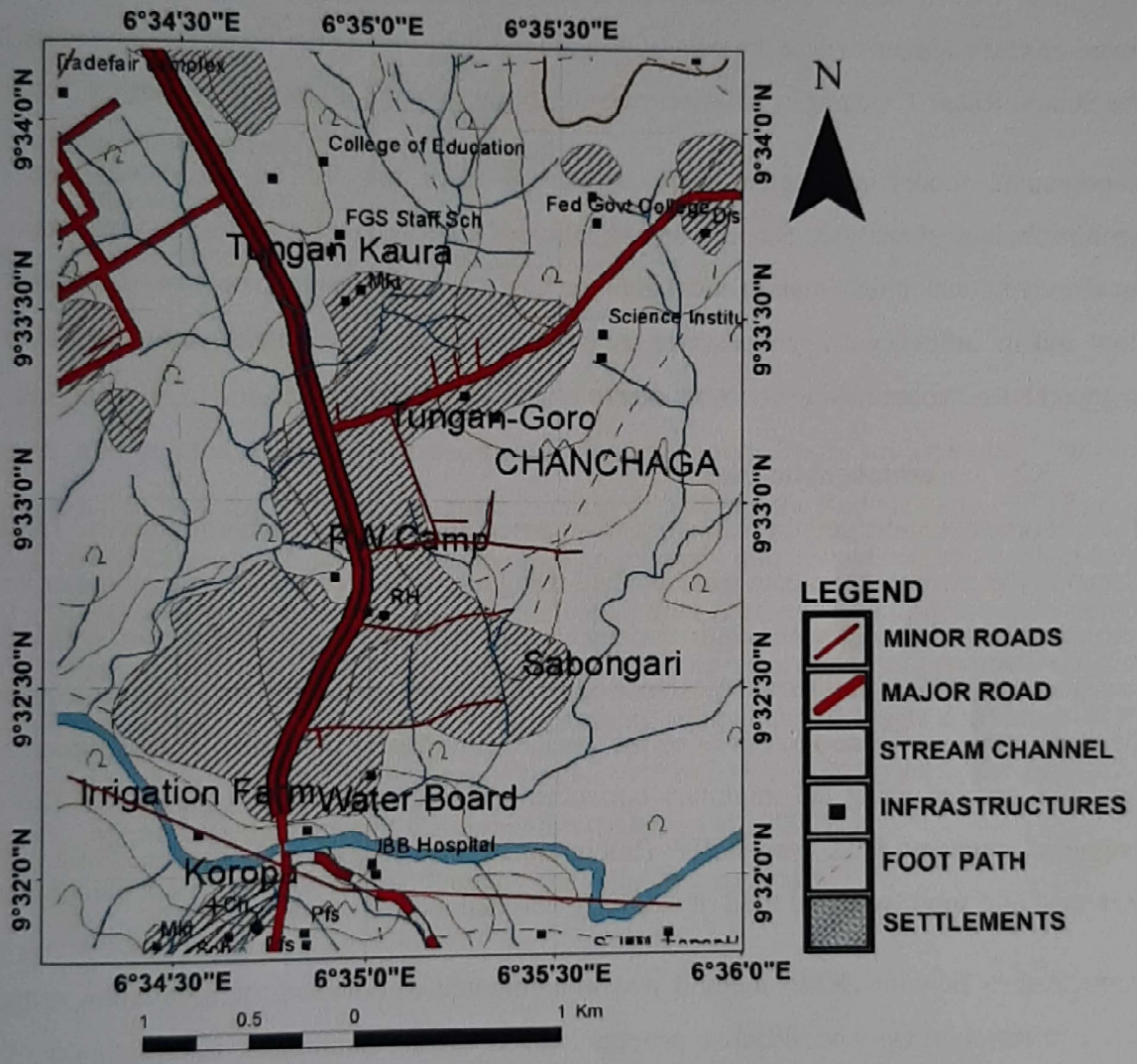

Figure 1: Location map of part of Minna Sheet 164SW.

3.0 MATERIALS AND METHODS

Lithologic and Surface Structural Data

The topographic map of 1:50,000 Sheet 164 (Minna) was digitised and transformed into 1:25.000 topographic map. This then was divided into 32 grid units of equal geographic coordinate intervals to help in achieving systematic surface geological mapping of the study area. Geographic Positioning System (GPS) device was used to record geographic coordinates and elevations. Strike and dip of outcropping foliated metamorphic rocks were measured with

compass clinometer. Structural information for fractures and joints were investigated in several rock outcrops. Lithologic descriptions of the various outcrops were also made.

3.1 SRTM DEM

The 30 m SRTM data was downloaded from http://dwtkns.com/srtm30m/. This site is an interface that attempts to ease the pain of downloading 30-meter resolution elevation data from the Shuttle Radar Topography Mission website (https://www2.jpl.nasa.gov/srtm/).

Topographic model parameters were calculated from the SRTM DEM and used for geomorphological analysis. Slope is an indication of the topographic setting as it relates to the local and regional relief situation and it gives an idea about the general direction of groundwater flow and its influence on groundwater recharge and discharge. The slope amount map (in degrees) was prepared using contours derived from SRTM DEM data.

3.2 Aeromagnetic Data

The airborne magnetic geophysical work was carried out by Fugro Airborne Surveys Limited, Canada. The aeromagnetic data was obtained using a proton precession magnetometer with a resolution of 0.01nT and were acquired along a series of NE-SW tie lines direction with a flight line spacing of 500 m and terrain clearance of 80 m. The micro-leveled magnetic data covering the study area was windowed out using the vertices coordinates in Oasis Montaj software. The data was gridded using the minimum curvature gridding method (Briggs, 1974). The total magnetic intensity field was IGRF (International Geomagnetic Reference Field, 2010) corrected and super-regional field of 32000nT was deducted from the raw data.

Reduction to Equator (RTE) method was implemented to position the anomalies vertically above their sources. The filtering process served to aid qualitative interpretation of the anomalies, while the depth analysis technique aided the interpretation of the subsurface magnetic anomalies quantitatively. RTE was implemented on the acquired aeromagnetic data with the objective of accurately positioning anomalies directly above their causative bodies. The geomagnetic declination and inclination of -2.03° and -4.73° respectively at the central location of the study area was used for the RTE process.

3.2.1 First Vertical Derivative (FVD).

First vertical derivative of the data was computed so as to make lineaments identification easier. This process suppresses deeper anomalies while enhancing shallow anomalies which are better suited for groundwater exploration in the study area. Second vertical derivative pursues this

effect further but higher order derivatives are associated with noise that makes interpretations ineffective (Garry, 1969).

The equation of the wavenumber domain filter to produce nth derivative is:

$$F(\omega) = \omega^n \quad (1)$$

where: F = vertical derivative

= wavenumber (radians/ground unit)

n = order of differentiation

Note: $= 2\pi k$ where k is cycles/ground unit.

3.2.2 Tilt Derivative

To determine structures (fault and folds), the contacts and edges or boundaries of magnetic sources, and to enhance both weak and strong magnetic anomalies of the area, the TDR filter was applied to both the Residual magnetic intensity (RMI) and the Reduce to pole (RTP) grid. The tilt angle derivative filter attempts to place an anomaly directly over its source. Verduzco et al., (2004) showed in their work that tilt derivative filter performs an automatic-gain-control (AGC) filter which tends to equalize the response from both weak and strong anomalies, hence, providing an effective way to trace out along striking anomalies. Tilt angle derivative (TDR) of RMI locates the edges of formations, especially at shallow depths by using the theory that the zero contours are the edges of the formation (Salem et al., 2007).

The magnetic tilt derivative is calculated by the following equation:

$$\text{TDR} = \tan^{-1}\left[\frac{dT/dz}{\sqrt{\left(\frac{dT^2}{dx}+\frac{dT^2}{dy}\right)}}\right] \quad (2)$$

where dT/dx is the calculated in-line gradient, dT/dy is the measured cross-line gradient and dT/dz is the measured vertical gradient of the total magnetic field.

3.2.3 Analytic Signal (AS)

The amplitude A of the analytic signal of the total magnetic field T is calculated from the three orthogonal derivatives of the field (Roest *et al.*, 1992).

$$|A(x,y)| = \sqrt{\left(\frac{\partial T}{\partial x}\right)^2 + \left(\frac{\partial T}{\partial y}\right)^2 + \left(\frac{\partial T}{\partial z}\right)^2} \quad (3)$$

where A = amplitude of the analytic signal

T = total magnetic field

x, y and z = orthogonal directions

Modelled grid of analytic signal was calculated by applying finite differences to the total intensity magnetic anomaly field computed from the formulas of Singh and Sabina, (1978). Vertical derivative of the magnetic field was obtained by computation at depths of $(z + \Delta x)$ and $(z - \Delta x)$ dividing the difference in the depths by $2\Delta x$. The x and y derivatives are calculated in the same manner. However, contacts on analytic signal is often more discontinuous than that of its horizontal derivative. The amplitude of the signal peak of analytic signal is directly proportional to the edge of magnetization. Hence source edges are easily determined.

3.3 Lineament extraction from SRTM DEM

Different visualization methods, especially shaded relief representations were used to enhance terrain features to support lineament extraction. The two main inputs provided for creating a hill shade map are the sun elevation angle (angle from the horizon) and the sun illumination angle or azimuth (orientation of the sun's rays with respect to north). Sun elevation angle of 30° was selected as lower sun angles are more effective in enhancing subtle topographic changes which in turn enhances linear features. The lower sun angle increased shadow effects, thus increasing the ease of lineament identification. Varying the sun illumination angle promotes identification of more lineaments on the different views of the same area since the lineaments orthogonal to the illumination angle are enhanced. Sun illumination directions of 0°, 45°, 225°, 270° and 315°, perpendicular to the prominent lineaments in the region, were selected to enhance the linear features. The lineaments so extracted were further analysed, processed and interpreted.

The lineaments from different hill shaded images of the SRTM DEM were digitised separately and subsequently combined to form a composite lineament for the SRTM DEMs This represents surface lineament map of the study area and the information was subsequently plotted as a Rosette diagram to allow for further analyses.

3.4 Lineament Extraction from Aeromagnetic Data

The lineaments were drawn from visual inspection on the computer screen using the computer's mouse on the shaded relief image of the total intensity magnetic anomaly map, FVD and Tilt derivative maps. The qualitative interpretation of the lineaments was carried out by visually inspecting the different versions of the geophysical maps at different scales and by digitizing the orientation of each interpreted lineament. All zones of magnetic minima as well as displacements/discontinuities of magnetic anomalies were digitized. The magnetic

lineaments were superimposed afterward as a separate layer. Because of parallax effects on the on-screen image, some lines may not be located exactly where they would be had it been they have been drawn on a smaller scale map and digitized.

3.5 Lineament Analysis

Lineaments from both datasets were integrated to form a composite lineament of the study area. The statistical analyses of the lineaments in the present study were based on the length and total number of the lineaments. The maximum, minimum and average length as well as the standard deviation of the length of the lineaments were also analysed. Rose diagram analyses were generated to show the orientation distribution of the lineaments. Rockworks 16 (RockWare) software tools were utilized to construct rose diagrams.

3.6 Source Parameter Imaging (SPI)

The SPI method (Thurston and Smith, 1997) estimates the depth from the local wavenumber of the analytic signal using the MAGMAP extension of oasis Montaj software. Thurston and Smith, (1997) and Nabighian (1972) showed that the analytic signal of the magnetic anomaly due to a 2D magnetic source can also be expressed by the complex number

$$A_1(x, z) = \frac{\partial B_T(x, z)}{\partial x} - j\frac{\partial B_T(x, z)}{\partial z}, \tag{4}$$

Where: B_T (x, z) is the total magnetic anomaly observation point at a distance x along the principal profile and a vertical distance z above the source

j is the imaginary number $(= \sqrt{-1})$.

A database of the various depth sources was created for every 250 m^2 of the entire study area. The results from the SPI method were compared with that of the spectral depth analysis method.

3.7 Hydrogeologic mapping and surface geophysical investigation

The static water level and total depth of about twenty-seven randomly selected hand-dug wells within and around the study area were measured using a graduated tape and a Garmin Global Positioning System (GPS) device for location marking and position heightening. The hydrogeological mapping was undertaken during the dry season (March) and hence, the static water level measurements from various wells represented the lowest level of static water table. Flow net was constructed using Surfer 13 software. This map is crucial for evaluating potential sources of groundwater as well as potential sources of groundwater contamination. It is also used in the understanding groundwater-surface water interactions.

VES profiles were constructed using results from extracted lineaments in the study area (Figure 2). The profiles were placed orthogonal to the directions of extracted lineaments. A total of thirty VES soundings were carried out using Schlumberger configuration with a view to determining the subsurface layering, overburden thickness, thicknesses of the aquiferous layers and the degree of fracturing of the bedrock. The acquired field data were converted to apparent resistivity values by multiplying with the appropriate Schlumberger geometric factor. The sounding curve for each point was obtained by inputting the data in WINRESIST software for iteration, modelling and output.

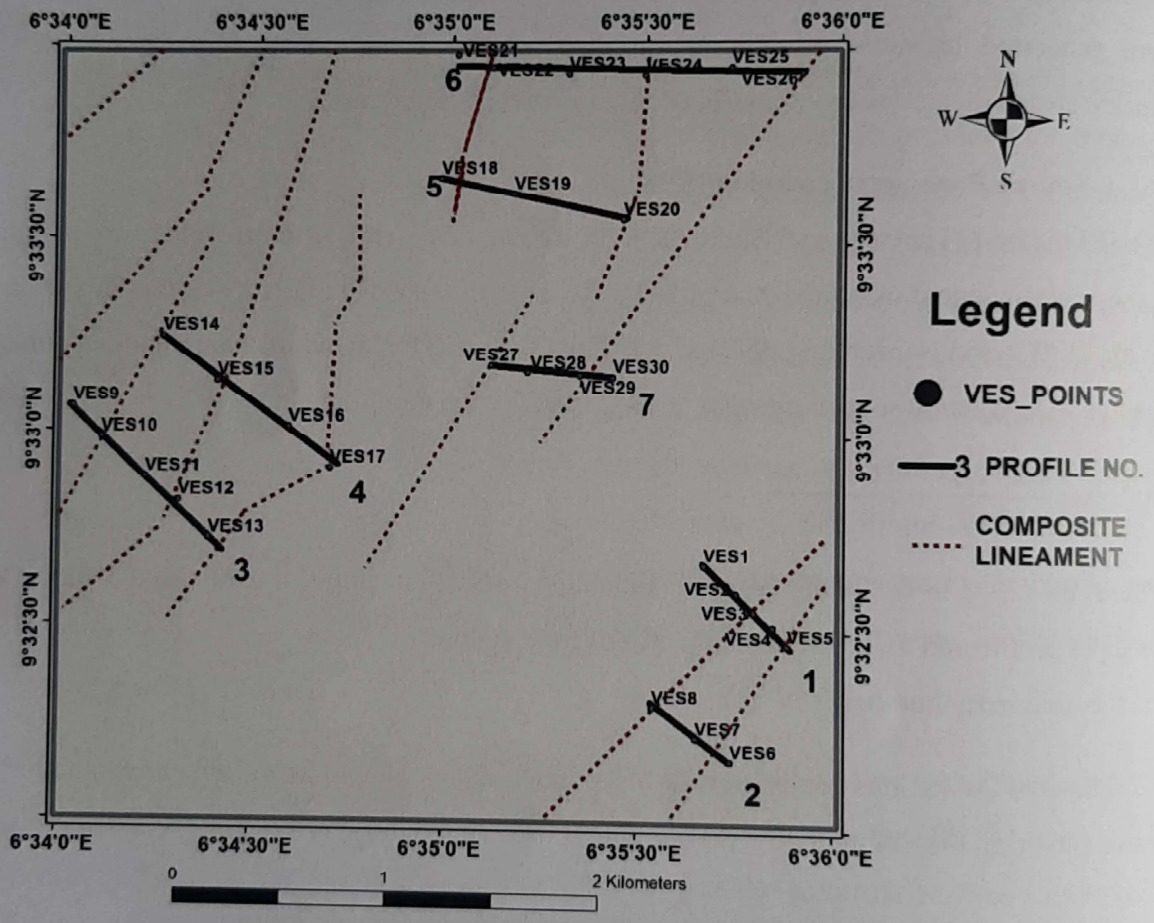

Figure 2: Structural map of part of Minna Sheet 164SW

3.8 Groundwater potential evaluation modelling

All thematic layers were reclassified to a common scale of 1 to 4 by intervals of 1, called scale values for the weighted overlay operation, with 4 being the highest potentiality score, 1 being the lowest, and 0 being restricted (unsuitable) values. The ArcGIS Weighted Overlay tool requires integers for the scale values, which were calculated by multiplying the grading values by 4 and rounding to the nearest integer. These scale values were used as the suitability scores.

The modelling involves delineation of groundwater potential zones based on five thematic maps which include lithology, slope and other derivative maps from vertical electrical sounding data. These derivative maps included overburden thickness, weathered layer isoresistivity, anisotropic coefficient and transverse resistance maps. The characteristic geoelectric parameters enabled the groundwater rating at each VES location following the methods of Olayinka et al., 1997). Every class in the thematic layers were placed into the very good, good, moderate or poor categories depending on their groundwater potential level.

3.8.1 Criteria A: Lithology

The values assigned to the lithology layer take into account the hydrogeological significance of the rock types. The characteristics considered for lithology are: rock type and fracture density. For instance, Migmatite rocks were adjudged to have better groundwater accumulation than other rock types due to the prevalence of joints and foliations.

3.8.2 Criteria B: Slope

Geomorphological parameters delineated in the study area were classified into five and values were assigned according to the type of landforms. For instance, channels and planes were considered better targets of groundwater occurrence and thus given higher weights. Conversely, ridges and peaks were assigned lower weights since they are judged not be adequate for groundwater accumulation. The slope angle map that was produced has the following slope classes: Class 1 (>14) °, Class 2 (7.1 – 14.0) °, Class 3 (4.1 – 7.0) ° and Class 4 (0 – 4.0) °.

It is obvious that the weighted values assigned for slope decreases as slope increases. This signifies that smoother topography presents more likelihood for groundwater accumulation.

3.8.3 Criteria C: Overburden thickness

The overburden thickness map has weights assigned to them which are directly proportional to the overburden thicknesses. These range from a minimum of 1 for thicknesses less than 5 m to a maximum of 4 for overburden thickness exceeding 15 m.

3.8.4 Criteria D: Weathered layer resistivity

The electrical resistivity of the saprolite layer overlying the basement is controlled by the parent rock type, climatic factors as well as clay content. a low resistivity of the order of less than 20 Ωm is indicative of a clayey regolith (Carruthers and Smith, 1992, Olayinka et al., 1997). This

reduces the permeability and thus lowers the aquifer potential. Weights were assigned to the weathered layer resistivity values according to Wright, (1992).

3.8.5 Criteria E: Bedrock resistivity

If the bedrock has low resistivity, a high aquifer potential could be inferred as a result of expected high fracture permeability. Maximum weight was assigned to cases where the resistivity of the bedrock is less than 750 Ωm. As the resistivity of the bedrock increases, there would be a reduction in the influence of weathering, with a corresponding lowering of the aquifer potential with bedrock resistivity.

3.9 Field Investigations (Ground Truthing)

Field investigation was done so that accurate correlations may be made with structural data obtained in the field and lineaments delineated from the remotely sensed data and the aeromagnetic data. Priority was given to those areas that have prominent anomalies, contact locations and lineament coincident regions.

4.0 RESULTS

4.1 Geology

The geology of the study area is shown in Figure 3. This is the geological map that was produced from the geological fieldwork. The exposed lithologic units comprised alluvial deposits, porphyritic biotite and biotite hornblende granite, fine to medium grained biotite and biotite hornblende granites. Others include foliated granite/granite gneiss, migmatitic gneiss/banded gneiss and migmatites.

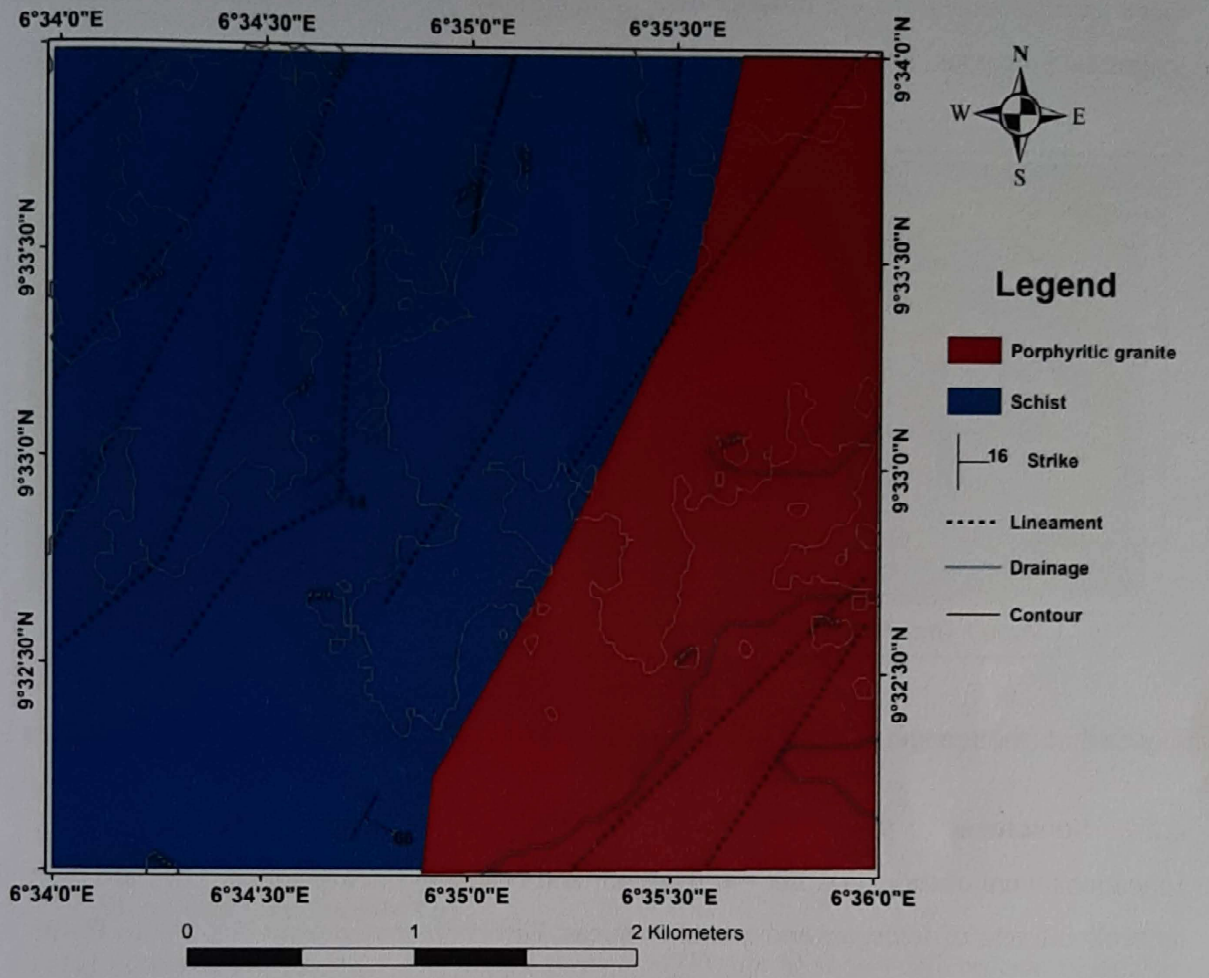

Figure 3: Geological map of part of Minna Sheet 164SW

These rocks have been reported to have suffered heterogeneous deformation as evident by migmatization and intrusion of large volumes of granitoids (Dada, 2006). Foliations give a dominant general trend of almost N-S and NE-SW. This is consistent with the regional trend ascribed to the structures produced by transcurrent movement and shearing (Olasehinde *et al.*, 1990). The rocks which are reasonably jointed generally show two joint sets trending NW-SE and NE-SW with the NW-SE being the more prominent. These granite bodies show a variation in the height of the outcrops which range from steep hills to low lying massive stock with gentle elevations, with textures ranging from fine to coarse.

Field evidence show that these rocks are not a homogeneous granite body but that only certain portions appear granitic in texture as evidenced by some gneissose texture (Plate II). Also, quartzo-feldspathic veins appear to thoroughly run through these rock bodies in almost all directions but most prominently in the horizontal and vertical directions. It is proposed that

these granite bodies are the product of a metamorphic process, metasomatism, rather than magmatic processes. The mineralogical composition is made

Figure 4: A photograph of some of the rock types mapped in the study area.

4.2 Structures

Lineations were observed on fine- to medium- and coarse-grained granites. They are defined by broken linear of feldspars and quartz or micas. Directions range from NE-SW to E –W. In gneiss, the dominant foliation trend is NE-SW, defined by the parallel arrangement of clustered mica flakes. In banded gneiss, the gneissose foliation is well defined by compositional segregation of mafic and felsic mineral components of the rock. The foliation is further accentuated by the alternating parallel bands of paleosomes and neosomes. Both foliations are commonly parallel.

Few minor transcurrent faults were seen. A fractured quartz vein with a dextral displacement of 4 mm and 040^0 fault axis was observed in coarse-grained granite. The joints in granites have predominant NE-SW and NW-SE trends (Plate I). Some of the rocks have undergone a level of physical weathering process resulting into exfoliation. Some of the coarse grained granitic rocks exhibit closely spaced jointing (Plate I). The porphyritic granites typically form highlands in the area with spheroidal boulders on the surface. A Rose plot of these measurements is presented in Figure 5. The principal joint directions trend NW-SE. Minor joint directions trend NE-SW.

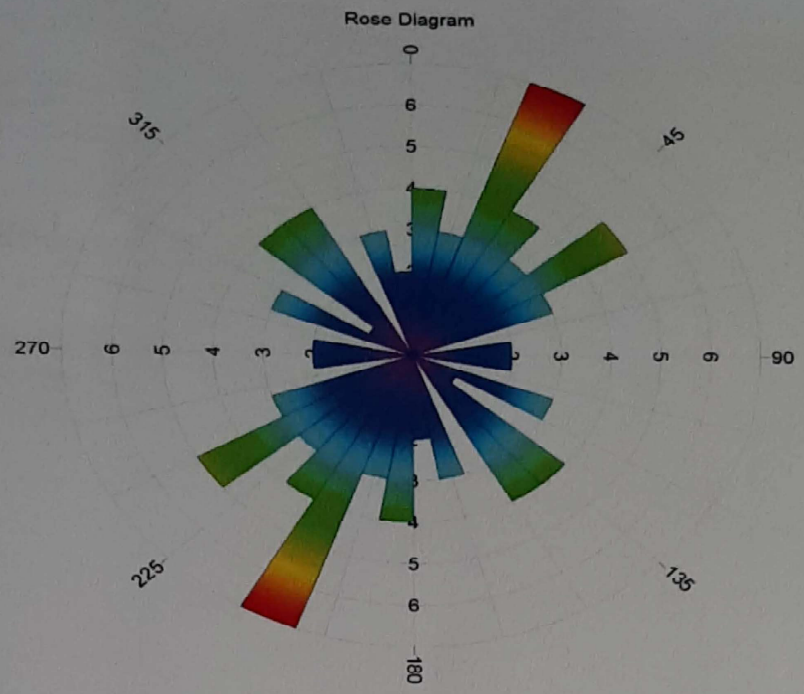

Figure 5: Generalised Rose Plot showing trends of joints on exposed rock surfaces in the study area.

4.3 Slope and Geomorphology

The colour shaded slope angle map of the study area (Figure 6) shows different range of slope angles in different colours. Slope angle amount vary from less than 1.5 degrees to slightly above 31 degrees. Areas having slope amount values of less than 1.5 degrees (dark green) imply a nearly flat surface. Slope angle amount values between 1.14 to 3.38 degrees (light green) show areas having very gentle to gentle slopes. Slope angle amounts with values ranging from 3.39 degrees to 7.5 degrees (yellow) and 7.5 degrees to 13.90 degrees (brown) show areas with slightly steep and steep slopes respectively. Slope angle amount values that are greater than 13.91 degrees (red) signify areas with very steep slopes.

In relation to groundwater potential, flat areas where the slope amount is low are capable of holding rainfall, which in turn correspond to recharge zones whereas in elevated areas where the slope/gradient amount is high, there will be high runoff and low infiltration. The steeper the slope, the greater will be the runoff and thus, lesser is the groundwater recharge.

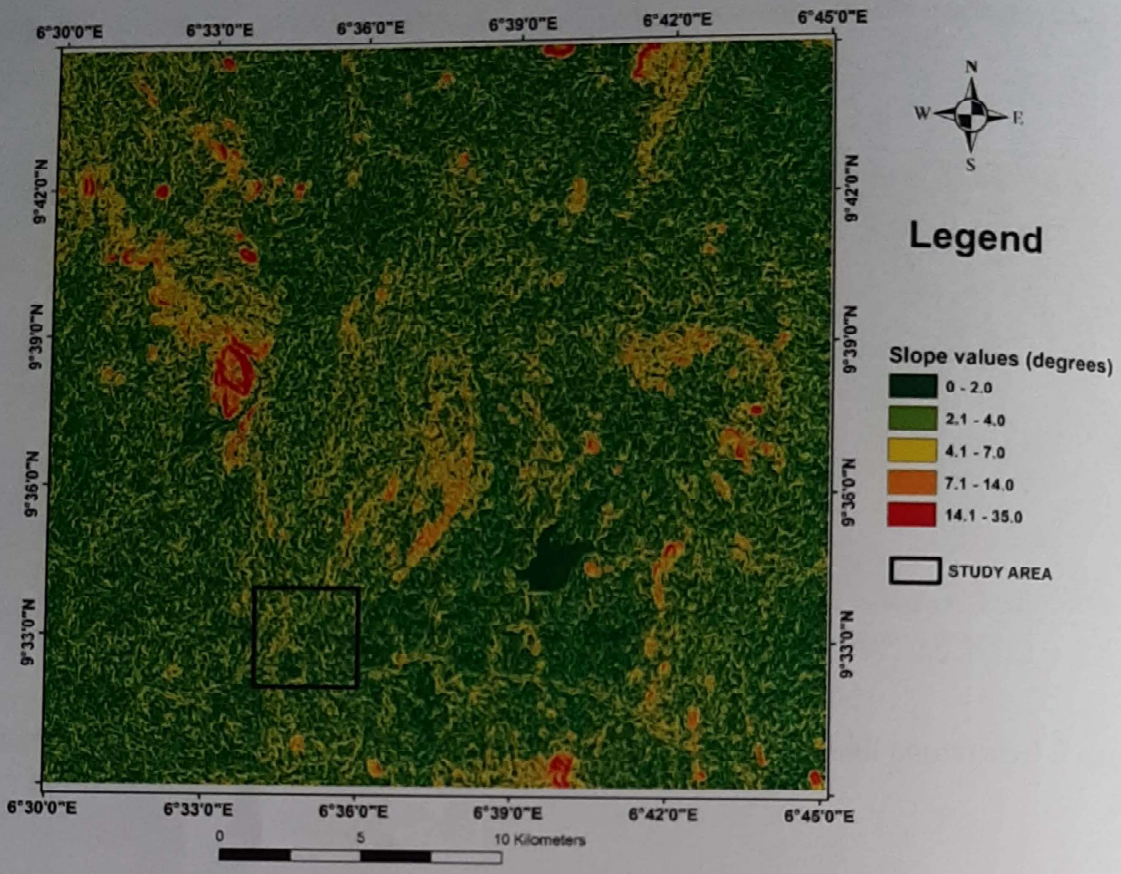

Figure 6: Slope angle map of 1:100.000 Sheet 164 (Minna) (Study area in black square)

4.4 Lineament extracted from SRTM images

Lineaments extracted from remotely sensed imagery are oriented predominantly in the NE–SW directions These lineament directions correlate well with joint directions mapped on the surface. In addition, these lineaments correspond to alignment of stream segments implying a form of structural control of the drainage system the NE–SW trending structures are parallel to the Pan-African regional tectonics. This deformation event is closely related to the formation of the schist belts and mylonites in the region have attributed NE–SW trend (Ajakaiye *et al.*, 1991)

4.5 Aeromagnetic Data

4.5.1 Qualitative Analysis of the Total Magnetic Intensity Map

The total magnetic intensity anomaly map (TMI) of the study area is presented in Figure 7. The colour of the residual TMI map range in values from magenta as high to blue as low. Residual magnetic intensity values range from -108 nT to 80 nT. The study area is dominated by NE-SW trending high and low magnetic anomalies. When compared with the geological map of

the area, the magnetic anomalies trend in the same direction with the regional geological structures (lineaments) in the area and the surface joint system of the area. a comparison of these anomalies with the geologic map of the study area show that the high magnetic anomalies represent the granitic rocks while the lower magnetic intensity anomalies represent areas underlain by schistose rocks.

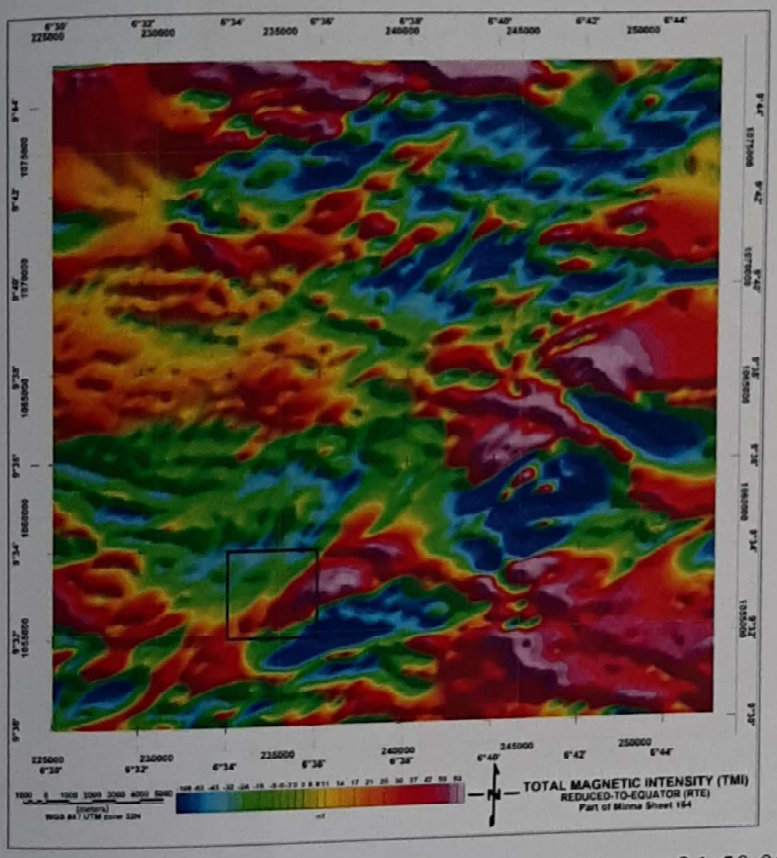

Figure 7: Total Magnetic Intensity Anomaly map of 1:50,000 Sheet 164 (Minna) processed using Oasis montaj on data obtained from NGSA.

4.5.2 First Vertical Derivative (FVD)

The FVD map aided in sharpening the edges of magnetic anomalies and also provided better resolution of their location. The FVD filter helped decrease broad and more regional anomalies and rather enhanced local magnetic responses which are interpreted as structures in the area. Most of the structures delineated in the area coincided with already delineated structures in the geological map of the area. The lineaments, where they are well defined, follow lithologic contacts. NE– SW trending fracture trends were seen to offset these lineaments. The NE – SW trending fractures were preserved in TMI map (Figure 7).

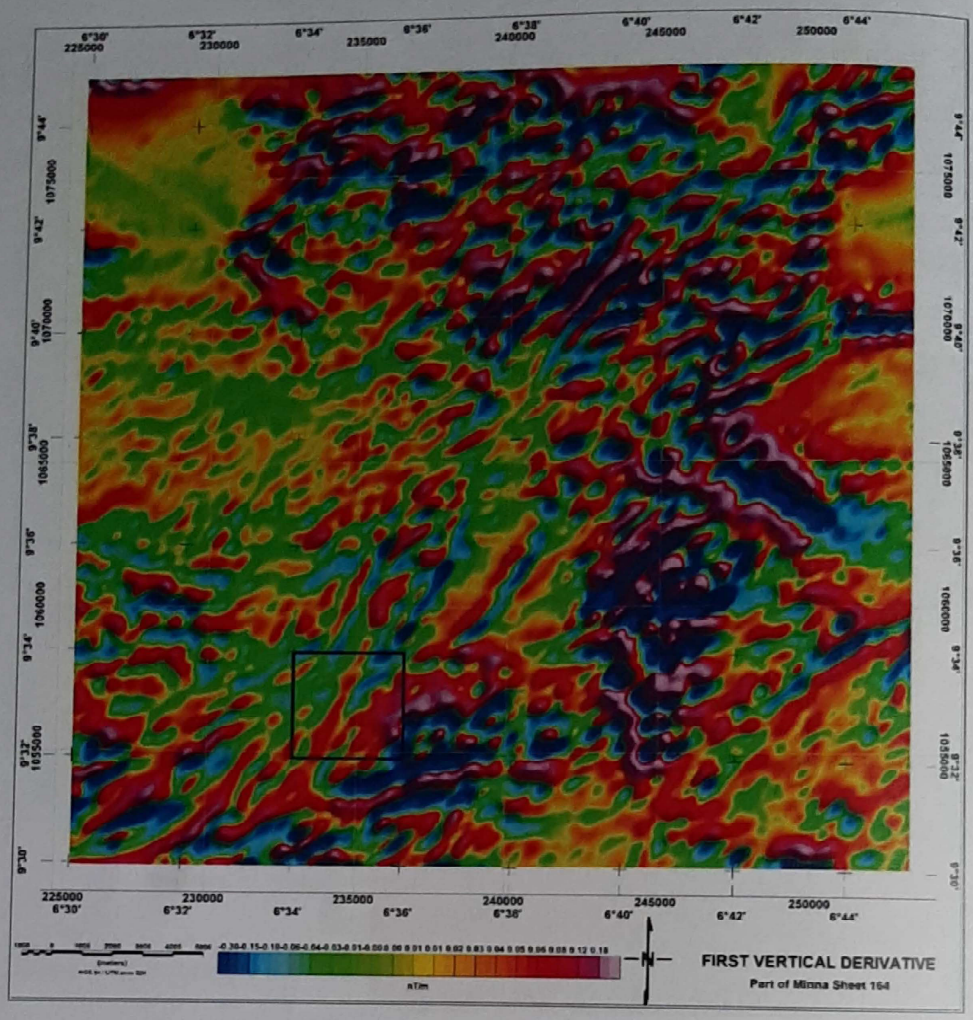

Figure 8: First Vertical Derivative map of 1:50,000 Sheet 164 (Minna) processed using Oasis montaj on data obtained from NGSA.

4.5.3 Tilt Derivative

It is observed that the zero contours estimate the location of abrupt changes in magnetic susceptibility values. The zero contour lines in this grid are represented by a yellow colour. Some structural lineaments were delineated by observing the abrupt change between the positive and negative magnetic anomalies (Figure 9). In Figure 8, a lot of noise believed to be from the shallow surface are observed which show that applying TDR on RTE on dataset from the study area can really help in delineating geology (lithology) and structures.

The geological meaning of a deformation zone, indicated by a lineament, may be estimated from the relation of the lineament to other magnetic patterns: Features crosscutting the magnetic anomalies are supposed to be younger than the magnetic sources and predominantly brittle in character, whereas concordant features are supposed to be more ductile. However, the geological observations from the Minna area show that due to the complex deformation history

of the bedrock, the classification of the lineaments using this method may be ambiguous: Many of the old ductile zones have been repeatedly reactivated, showing a semi-brittle and/or brittle character within the same zone. The comparison of the lineaments and direct geological observation suggests that from the different data sets, magnetic lineaments most likely present brittle deformation zones (Airo, 2005).

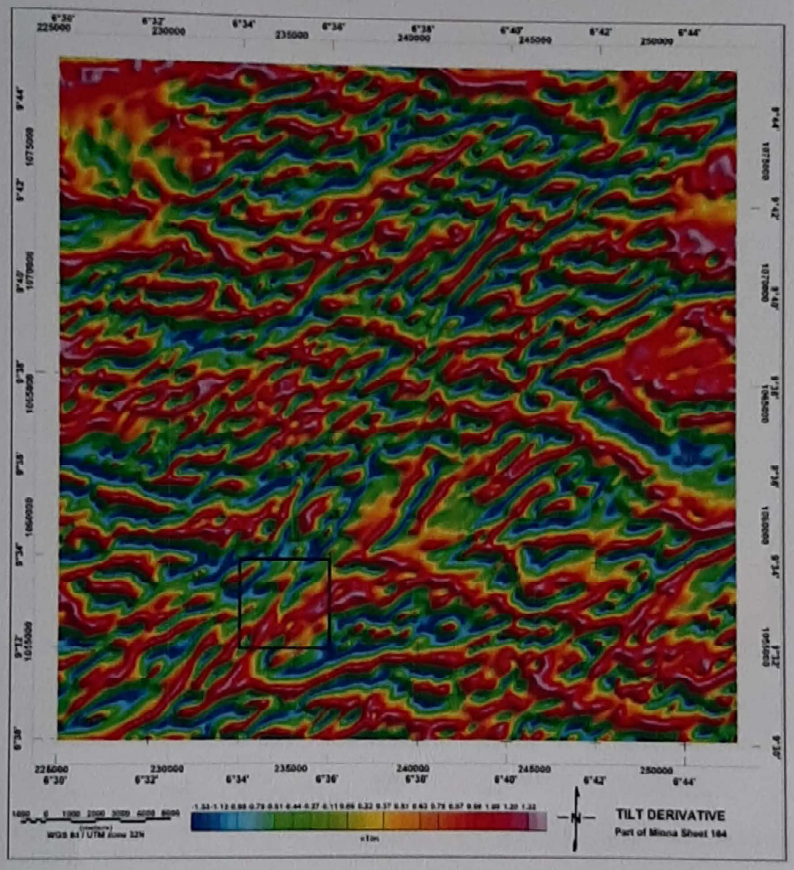

Figure 9: Tilt Derivative map of 1: 50,000 Sheet 164 (Minna) processed using Oasis montaj on data obtained from NGSA.

4.5.4 Source Parameter Imaging (SPI)

Figure 10 is a map of the depth estimates obtained from the source parameter imaging (SPI) processing technique. The depth estimates range from 100 m to over 400 m. The result from SPI process has a high degree of correlation with the result from spectral depth determination. Shallow regions from both methods correspond to the Basement Complex areas. Also, the results from the depth estimates agree with published works referred to in the literature review. It should be noted that only shallow depths of not greater than 150 m is considered adequate for groundwater development in this area (Ejepu, 2017). The depth of causative sources as interpreted from SPI map show that areas within the schist are shallower than areas within the

granites (Figure 10). Since intersection of lineaments is an indication of fracturing, it is expected that these are promising sites for groundwater accumulation. Also, relatively deep sections within the area are attributable to areas where deep weathering may have occured. These areas should have considerable contribution to groundwater availability.

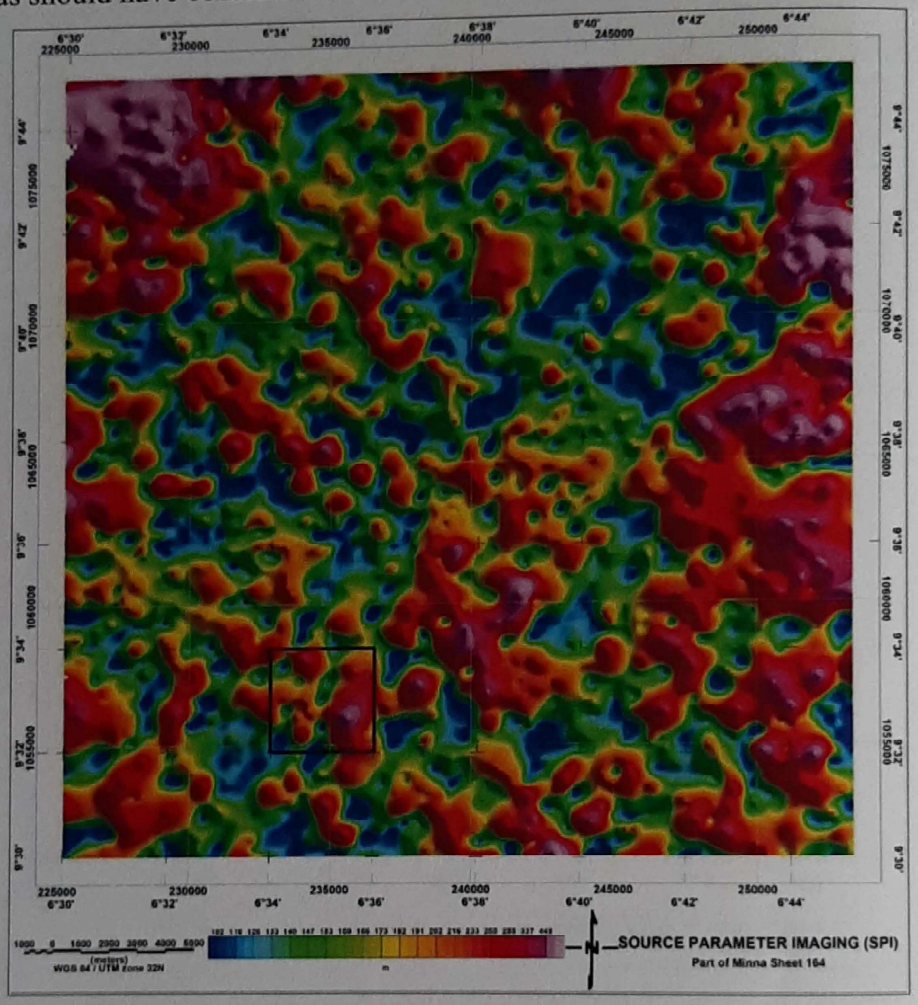

Figure 10: Source Parameter Imaging (SPI) map of 1: 50,000 Sheet 164 (Minna) processed using Oasis montaj on data obtained from NGSA.

4.6 Hydrogeological mapping

Hydrogeological mapping was conducted as part of the methods incorporated in the exploration of groundwater in the area. Static water levels obtained from wells surveyed ranged from 217 to 268 m. this was used to construct a vector map using surfer to indicate possible groundwater flow directions. From the groundwater flow direction map (Figure 11), the d irection of flow is mainly towards the southern part of the map. this convergence zones are zones of high groundwater potential.

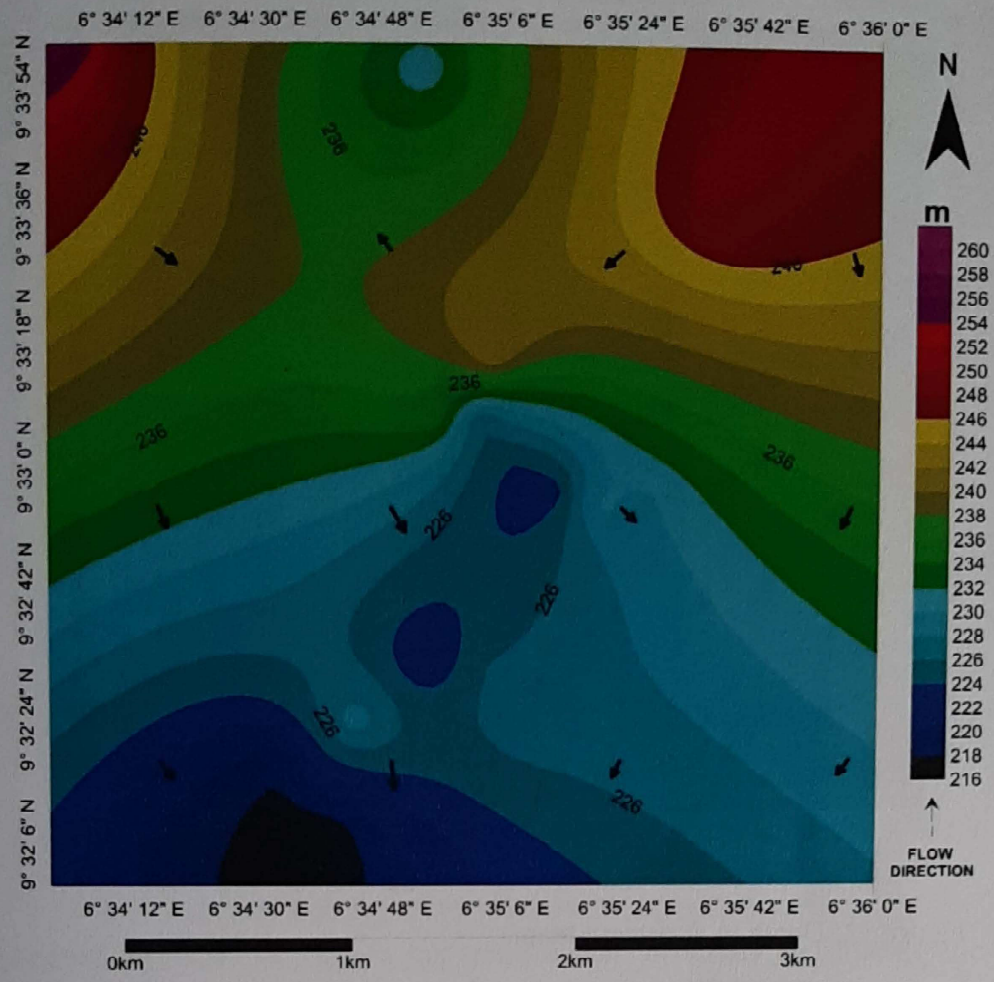

Figure 11: Groundwater flow map showing direction of flow

4.7 Vertical Electrical Sounding Data

The depths to basement (overburden thickness) beneath the sounding stations were plotted as shown in figure 12. this was done to enable a general view of the aquifer geometry of the surveyed area. the overburden is assumed to include the top soil, the lateritic horizon and the weathered rock layers. the values range from 2 m to 36 m. areas with thick overburden corresponding to basement depression and are known to have higher groundwater potential particularly in the basement complex terrains (Olorunfemi and Okhue, 1992).

the northern and south-eastern portion of the map generally have low overburden thicknesses. the south-western and north-western portions of the map generally has high overburden thicknesses.

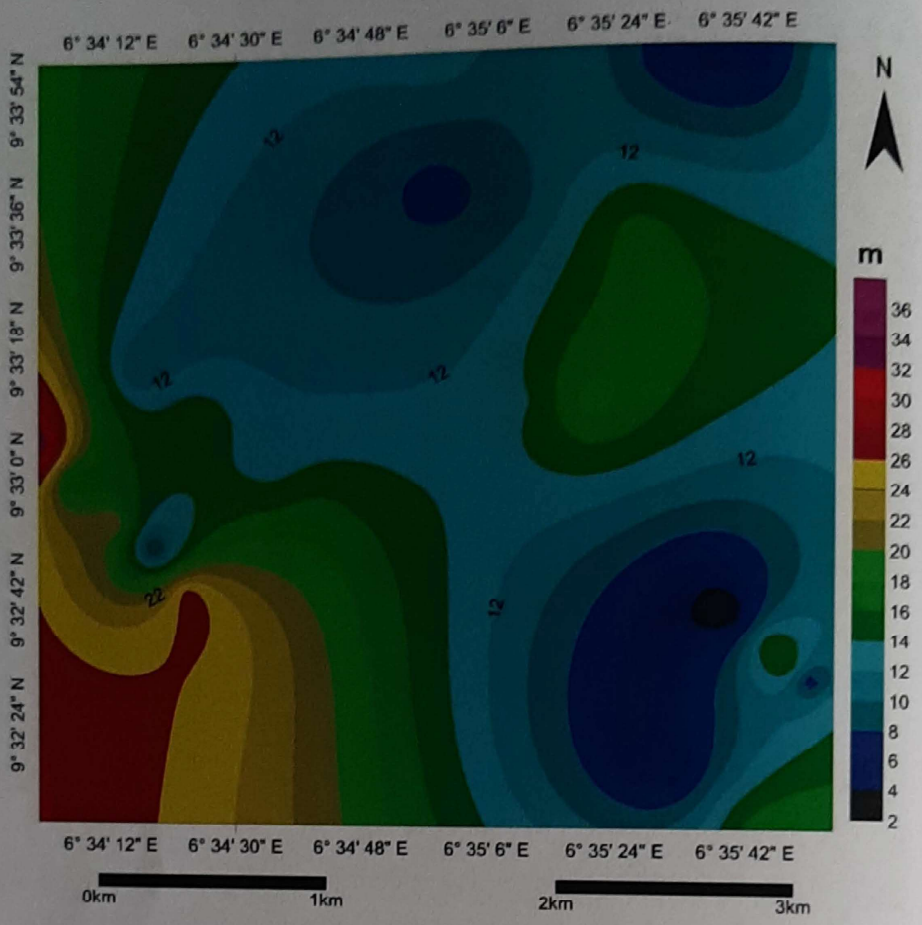

Figure 12: Depth to Basement map

The weathered layer isoresistivity map (Figure 13) was produced in order to distinguish high water bearing weathered layer from low water bearing ones. also, the map was produced to determine if the degree of weathering or saturation varies from point to point in the study area. the resistivity of the aquifer is highest at the northern and the north-western portion of the map. the high resistivity values associated with these parts is possibly due to the almost sandy nature of the aquifers. Generally low resistivity values observed in the map are probably due to the highly weathered nature of the weathered basement layer which sometimes may tend towards clay as can be seen in the north-eastern portion of the map.

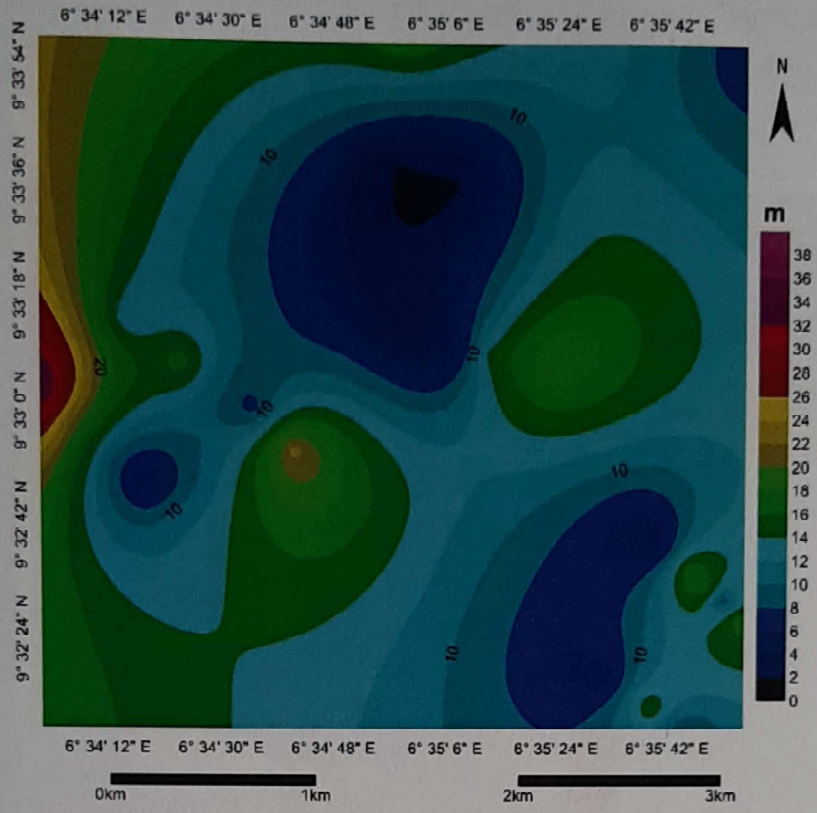

Figure 13: Weathered layer isoresistivity map

The weathered layers as defined in this research are materials constituting the regolith, straddled in-between the top soil and fractured/fresh bedrock. the thickness of these lithological materials varies between 2 m and 40 m. this was determined from the layer interpreted values of the sounding results

Resistivity values of the bedrock vary from 200 Ωm to over 10000 Ωm. the area generally has high bedrock resistivity.

Seven curve types were generated from the VES analysis namely: QH, HK, Q, K, H, A and KH portraying various aquifers within the region. The H-type covers 63.3%; the A-type and Q-type covers 10%; the K-type covers 6.66%, while the remaining 3.33% of the total surveyed points is covered by the HK-type, QK-type and KH-types. The groundwater yield in these areas could not be very high because the density of the fractured column is not high (Olorunfemi, 2009). The HK curve-type areas may not have hydraulic connectivity between the fresh rock and the weathered rocks because of the fractured zones are underlained after the fresh rock zones, this on another view will help to improve upon the recharge of a sunk well in such areas, especially in an area where both zones (fractured and fresh rocks) have thick layers. The KH curve-type are areas where top soil is generally of thin layer and also the fractured layer is

confined in the fresh basement too. Significant yield of water is possible when the fracture density is high with a high fracture column thickness too.

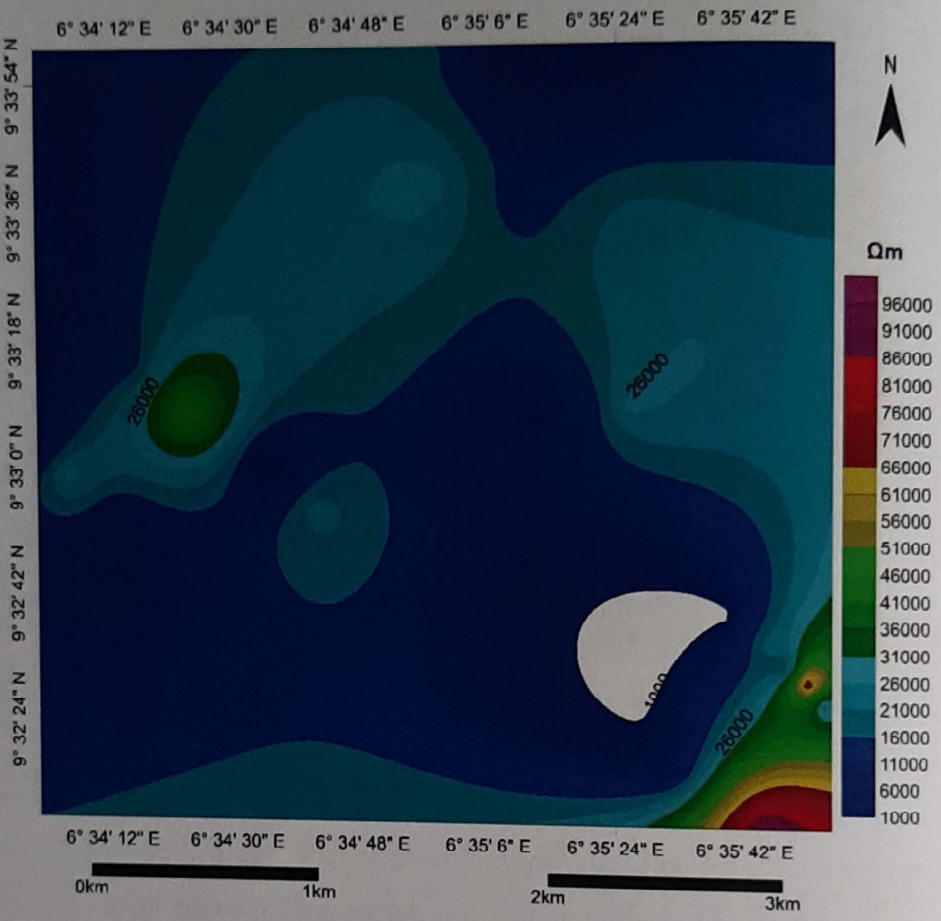

Figure 14: Bedrock isoresistivity map

The areas marked by QH curve-types have sharp transition between the weathered and the fresh basement, in these areas, the weathered layer is the sole aquifer unit and groundwater yield here is determined by the degree of shaleliness of the weathered layer, low yield is obtained where underlain by schist or clay (Olugboye, 2008).

Figure 15 shows the groundwater potential map of the study area produced from integrating the geology, geomorphology and interpreted VES data. The different groundwater potential areas are depicted on the map.

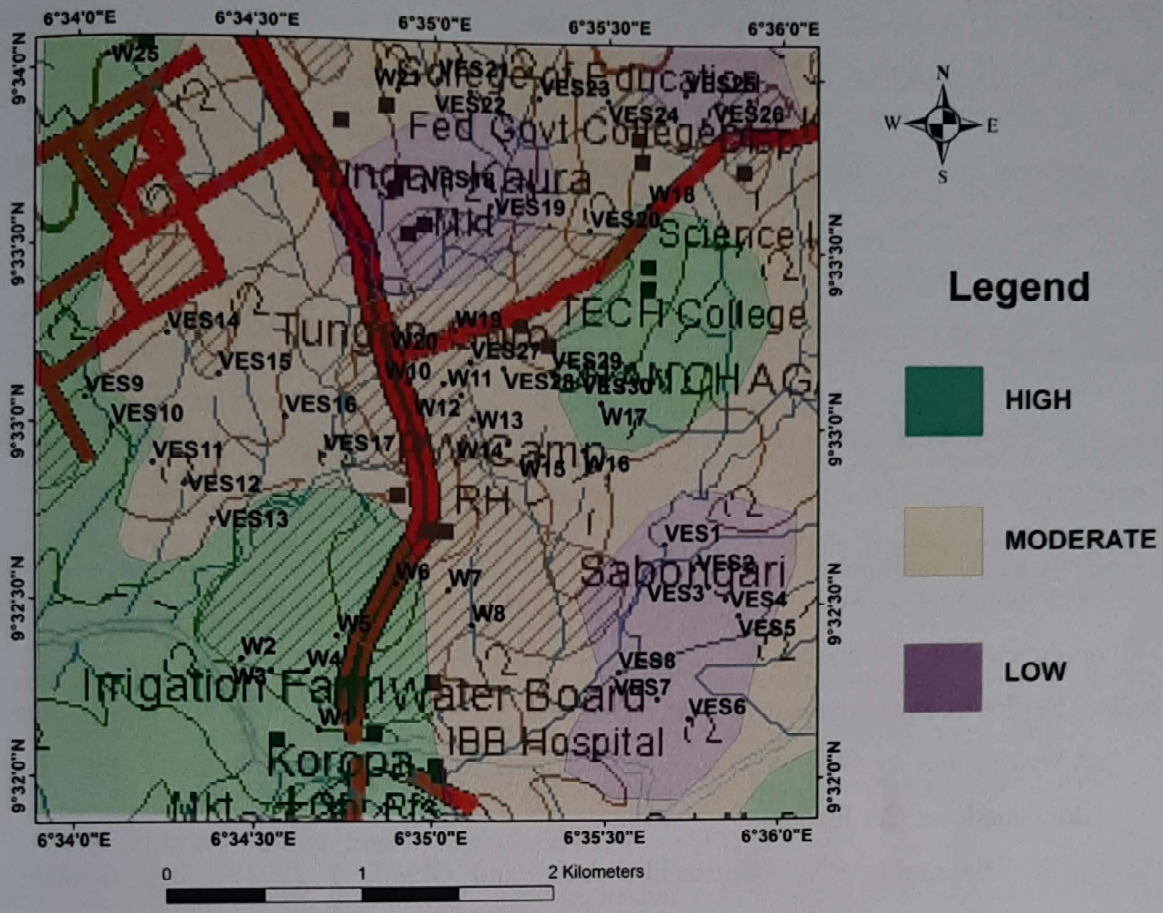

Figure 15: Groundwater potential map of the area

4.8 CONCLUSION

Aeromagnetic and SRTM data in combination with Vertical Electrical Sounding have been utilised to unravel the structural orientations of the study area. This permitted the informed decision to align VES profiles normal to these prominent orientations for optimal delineation of fractures that would improve borehole drilling success rates. Geologic mapping revealed that the study area is underlain by granite located in the eastern part and schist in the western part of the study area. Structural measurements obtained during field mapping reveal principal joint directions trending NE - SW direction. Interpreted Vertical Electrical Sounding (VES) reveal predominantly H-type sounding curve. Top soil thickness range between 1 m and 7 m while the weathered layer range in depths of 3 m and 37 m. The thick weathered portion enhanced well yields. Groundwater potential map of the area is demarcated into high, medium and low groundwater potential zones. The high groundwater potential zones may further be studied and investigated to bring about better yields for wells drilled in that portion of the study area.

REFERENCES

Airo, M. L. (2005). Regional interpretation of aerogeophysical data: Extracting compositional and structural features. In Airo, M. L. (Eds.), *Aerogeophysics in Finland 1972–2004: Methods, System Characteristics and Applications*. Geological Survey of Finland, Special Paper 39, 21–74.

Ajakaiye, D. E., Hall, D. H., Ashiekaa, J. A., & Udensi, E. E. (1991). Magnetic anomalies in the Nigerian continental mass based on aeromagnetic surveys. *Tectonophysics*, 192(1), 211-230.

Briggs, I. C. (1974). Machine contouring using minimum curvature. *Geophysics*, *39*(1), 39-48.

Carruthers A.M. and Smith I.F. 1992. The use of ground electrical methods for siting water supply boreholes in shallow crystalline Basement Terrains. In: Wright, E.P and Burges, W.G (eds.), *The hydrogeology of crystalline Basement Aquifer in Africa*. Special publication 66, Geological Society London. Pp 183-230

Dada, S.S. (2006). Proterozoic evolution of Nigeria. In Oshi O. (Eds.), *The Basement Complex of Nigeria and its Mineral Resources* (A tribute to Prof. M. A. Rahaman). (pp. 29-44). Akin Jinad and Co. Ibadan.

Ejepu J.S., Olasehinde P.I., Okhimamhe A.A., and Oknola I. (2017). Investigation of Hydrogeological Structures of Paiko Region, North-Central Nigeria Using Integrated Geophysical and Remote Sensing Techniques. Geosciences.

Ejepu, S. J., Olasehinde, P. I., Omar D. M., Abdullahi, D. S, Adebowale, T. A., & Ochimana, A. (2015). Integration of Geology, Remote Sensing and Geographic Information System in assessing groundwater potential of Paiko Sheet 185 North-Central Nigeria. Journal of Information, Education, Science and Technology. 2(1), 145 – 155.

Garry K.C.C. (1969). Optimum Second-Derivative and downward continuation filters. Geophysics 34 (3), 424-437.

Nabighian, M.N. (1972). The analytic signal of two dimensional magnetic bodies with polygonal cross-section, its properties and use for automated anomaly interpretation. *Geophysics*, 37, 507-517.

NIMET Seasonal Rainfall Prediction (2017). Retrieved from http://nimet-srp.com/2015-Annual-Rainfall-Predictions.html.

Olasehinde, P. I., Pal, P. C. & Annor, A. E. (1990). Aeromagnetic anomalies and structural Lineaments in the Nigerian Basement Complex. *Journal of African Earth Sciences*, 1(3&4), 351-355.

Olayinka, A.I., Akpan, E.J. and Magbagbeola, O.A. (1997). Geoelectric sounding for estimating aquifer potential in the crystalline basement area around Shaki, South West Nigeria, *Water Resources* 8(1 and 2) 71-81

Olorunfemi M.O., and Okhue E.T., (1992). Hydrogeologic and Geologic significance of a Geoelectric Survey At Ile-Ife, Nigeria Journal of Mining and Geology. Vol.28, No.2,221 - 229.

Olorunfemi, M. O. (2009). Groundwater exploration, borehole site selection and optimum drill depth in basement complex terrain. *Journal of water resources*, 2, 5 – 10.

Olugboye, M. O. (2008). *Hydrogeological Practices (with Application to Nigerian Groundwater Terrains)*. Ilorin. PIOS Publishers.

Roest, W.R., Verhoef, I. & Pilkington, M. (1992). Magnetic interpretation using the 3-D analytic signal. *Geophysics,* 57(1), 116 125.

Salem, A. Simon, W. Fairhead, D. Ravat, D, Richard, S. (2007). Tilt depth method: Asimple depth estimation using first-order magnetic derivatives. The leading-edge, 26, 12

Singh, S. K. & Sabina, F. J. (1978). Magnetic anomaly due to a vertical right circular cylinder with arbitrary polarization: *Geophysics,* 43, 173–178.

Thurston, J.B., & Smith, R. S. 1997. Automatic conversion of magnetic data to depth, dip, susceptibility contrast using the SPITM method. *Geophysics*, 62, 807–813.

Verduzco, B. Fairhead, J.D. Green, C.M. and MacKenzie,C. (2004). New insights into magnetic derivatives for structural mapping: The leading Edge, 23, 116-119

Wright, E. P. & Burgess, W. G. (eds) (1992). Hydrogeology of Crystalline Basement Aquifers in Africa. *Geological Society Special Publication* 66, 1-27.